

Synthesis and catalytic performance of organic-inorganic hybrid mesoporous material having basic nanospace

Tetsuya Shishido,*^a Toru Kawaguchi,^a Tomohito Iwashige,^a Kentaro Teramura,^b Yutaka
Hitomi,^c and Tsunehiro Tanaka*^a

Affiliations

^a *Department of Molecular Engineering, Graduate School of Engineering, Kyoto University,
Katsura, Kyoto 615-8510.*

^b *Kyoto University Pioneering Research Unit for Next Generation, Kyoto University, Katsura,
Kyoto 615-8510.*

^c *Department of Molecular Chemistry and Biochemistry, Doshishya University, Kyotanabe,
Kyoto 610-0321, Japan.*

Corresponding authors

Dr. Tetsuya Shishido and Prof. Tsunehiro Tanaka

Department of Molecular Engineering, Graduate School of Engineering, Kyoto University,
Nishikyo-ku, Katsura 1, Kyoto 615-8510, Japan.

Tel: +81 75 383 2559

Fax: +81 75 383 2561

E-mail: shishido@moleng.kyoto-u.ac.jp, tanakat@moleng.kyoto-u.ac.jp.

Abstract

Basic nanospace was synthesized by the homogeneous modification of FSM-16 with 3-(triethoxysilyl)pyridine, which is a rigid substrate without an alkyl chain as linker. Aldol condensation of butanal gave the corresponding dimer in high yields over 3-(triethoxysilyl)pyridine-modified FSM-16. A copper-pyridine complex was immobilized within the interior of FSM-16 using a modified pyridyl group as the ligand and the oxidative coupling polymerization of 2,5-dimethylphenol proceeded with high regio-selectivity.

Keywords:

FSM-16, basic nanospace, aldol condensation, regio-controlled oxidative coupling

1. Introduction

Mesoporous silicate such as M41S, FSM-16, and SBA-15 possesses uniform and well-ordered channels with controllable pore size from 2 to 10 nm and high surface area (ca. 1000 m² g⁻¹). Because of these unique characteristics, mesoporous silicate has received much attention in areas of catalysis, chromatography and adsorption [1-6]. Kageyama et al. reported that crystalline nanofibers of linear polyethylene were formed by the polymerization of ethylene with titanocene (Cp₂Ti where Cp is the cyclopentadienyl ligand) supported on mesoporous silica [7]. Lin et al. observed the high crystallinity polymers of 1,4-diethylbenzene by using MCM-41 [8]. Shibasaki et al. reported the regio-controlled polycondensation of 2,6- and 2,5-dimethylphenols using a copper-amine catalyst on SBA-15, whose pore size is ca. 6 nm, with an excess of additives such as pyridine and alkyl substituted pyridine [9,10]. These facts indicate that the uniform and well-ordered nanospace of mesoporous silica would be useful for controlling the orientation of molecules. In order to introduce active metals and metal oxides to mesoporous silicate, several kinds of methods such as direct hydrothermal, impregnation, grafting, and template ion exchange methods etc. have been reported. Recently, the organic-inorganic hybrid porous material has also attracted great attention. The introduction of organic groups into an inorganic network or surface

leads to new variation of structural properties, thereby promoting new potential applications for the resulting organic-inorganic hybrid materials [1-17]. For example, acidic [13-16] and basic [17, 18] materials have been immobilized in micro and mesoporous materials. When organic groups are introduced into a silicate mesopore, a heterogeneous modification to the pore surface and/or entrance is often obtained. This kind of heterogeneous modification leads to lack of uniformity in the distribution of pore size, resulting in the disappearance of effective characteristics of mesoporous material like uniform and well-ordered channels. Thus a new concept of homogeneous modification to the inside of a mesopore surface by organic groups is required.

Here, we demonstrate the synthesis of uniform and well-ordered basic nanospace by the homogeneous modification of FSM-16 with 3-(triethoxysilyl)pyridine (3-PySi(OEt)₃), which is a rigid substrate without an alkyl chain as linker. The basic property of FSM-16 modified with 3-PySi(OEt)₃ (Py_FSM-16) is tested by aldol condensation of butanal, which is one of the typical basic reactions [18]. The immobilization method of the copper-pyridine complex within the interior of the mesopore of FSM-16 and its novel catalysis in the oxidative coupling polymerization of 2,5-dimethylphenol without additives are also discussed.

2. Experimental

2.1 Preparation

Pure silica FSM-16 was prepared from kanemite according to a method previously reported [19]. As a silica source, high purity water glass (Fuji Silysia Chem. Co. Ltd.; SiO₂ =15.3 wt%, Na₂O=6.1 wt%, Al=0.6ppm, Fe=0.4ppn) was used. 3-(Triethoxysilyl)pyridine (3-PySi(OEt)₃) was synthesized according to the literature [20]. The pyridyl groups were anchored on FSM-16 (Py_FSM-16) by the post-modification method as follows: 3-PySi(OEt)₃ and FSM-16, which were previously evacuated at 473 K for 20 h, were refluxed in dehydrated toluene under a N₂ atmosphere for 24 h. After refluxing, the modified materials were separated by filtration, then washed with dry toluene, and evacuated at 353 K overnight. The quantity of pyridyl groups anchored on FSM-16 determined by elemental analysis was 1.47 mmol g⁻¹. The copper-pyridine complex was immobilized within the interior of FSM-16 by treating Py_FSM-16 with a ratio of 0.5 equivalent of copper chloride(I) to the pyridyl group in toluene. The resulting green powder was collected and dried under vacuum for 12 h.

2.2. Characterization

The nitrogen adsorption-desorption isotherm measurements were carried out using a BELSORP 28SA (BEL Japan) at 77K. Prior to the measurement, each sample was outgassed at 373 K for 1 h. X-ray diffraction patterns of the catalysts were recorded using a SHIMADZU XD-D1 X-ray diffractometer with Ni-filtered Cu K α radiation. FT-IR spectra were recorded using a Perkin Elmer Spectrum One instrument with a resolution of 4 cm⁻¹. ²⁹Si CP-MAS NMR spectra were recorded using a JEOL JNM-AL300WB spectrometer (45 MHz, CP-MAS technique with contact time of 2 msec) for observation of the change in the local environment of Si before and after modification of with 3-PySi(OEt)₃.

2.3. Catalytic reactions

The aldol condensation of butanal was carried out in an H-shaped glass batch reactor. 50 mg of sample was placed in one batch and outgassed at ambient temperature for 1 h and sealed. The known amount of butanal (7 mmol) degassed and passed through 3A molecular sieves was stored in the other branch until it was introduced through the breakable seal by distillation into the branch containing the catalyst thermostatted at liquid nitrogen temperature. Reaction was initiated by melting the reactant mixture at a reaction temperature followed by stirring. 50 mg of Py_FSM-16 is equivalent to 1.1 mol% of pyridyl group to butanal. The

conversion of butanal was quantified by using internal standard and the following equation (Eq. (1)).

$$\text{Conversion (\%)} = (\text{butanal}[\text{intial}] - \text{butanal}[\text{residual}]) / \text{butanal}[\text{initial}] \times 100 \quad (1)$$

The selectivities to dimer and trimer were quantified by using internal standard and decided on carbon basis.

Oxidative coupling polymerization of 2,5-dimethylphenol using 3 mol% of copper catalyst to the monomer was performed in toluene at 343 K under an atmospheric oxygen. The catalyst and a stirring bar were charged in a two-necked flask. The flask was purged with oxygen two times. The polymerization was initiated by the addition of 2,5-dimethylphenol and the solution was vigorously stirred at 343 K. After the reaction, the reaction mixture was centrifuged and filtered, then the filtered solution was poured into 100 mL of methanol to precipitate the polymer. The precipitate was collected, dissolved in chloroform, and reprecipitated with methanol. The polymer was evaporated and dried at 353 K. $^1\text{H NMR}$ spectra (400 MHz, JEPL ECX400) were recorded for the determination of the structure of polymer.

3. Results and discussion

XRD patterns for FSM-16 and Py_FSM-16 show characteristic low angle peaks attributed to d_{100} , d_{110} , d_{200} reflections assuming a 2D-hexagonal lattice at the same position. This indicates that the hexagonal phase of FSM-16 is maintained after modification with 3-PySi(OEt)₃. Figure 1 shows N₂ adsorption-desorption isotherms of FSM-16 and Py_FSM-16. N₂ adsorption of Py_FSM-16 gave a high surface area and type IV isotherm as well as FSM-16, indicating the presence of uniform and well-ordered 2D-hexagonal channels even after modification of FSM-16 with 3-PySi(OEt)₃. After the modification with 3-PySi(OEt)₃, the BET surface area ($1040 \text{ m}^2\text{g}^{-1} \rightarrow 863 \text{ m}^2\text{g}^{-1}$), inner specific surface area estimated by the t -plot ($901 \text{ m}^2\text{g}^{-1} \rightarrow 751 \text{ m}^2\text{g}^{-1}$), pore volume ($1120 \text{ mm}^3\text{g}^{-1} \rightarrow 645 \text{ mm}^3\text{g}^{-1}$), pore diameter estimated by the Barrett-Joyner-Halenda (BJH) method ($2.56 \text{ nm} \rightarrow 2.08 \text{ nm}$) were decreased, respectively. If the layer of the homogeneously modified pyridyl groups on the interior of mesopore of FSM-16 acts as a pseudo-pore wall and the pore structure is approximated by one-dimensional cylindrical geometry model, the inner specific surface area is proportional to the pore diameter. Indeed, the ratio of inner specific surface areas before the modification to that after the modification was 0.83 and give close agreement with the ratio of pore diameter (0.81). The expected rate of decline in the pore volume by the modification from this

one-dimensional cylindrical geometry model also corresponds with the experimental value. These results suggest that the layer of homogeneously modified pyridyl groups on the interior of mesopore of FSM-16 acts as a pseudo-pore wall.

The FT-IR spectrum of bare FSM-16 has a band at 3742 cm^{-1} as shown in Figure 2 (b). This band is assigned to the OH stretching vibration of isolated silanol group. After the modification, the band at 3742 cm^{-1} disappeared and new bands at 1403, 1477, 1570 and 1587 cm^{-1} assigned to the vibration of pyridine ring appeared (Figure 2 (c)). These results indicate that the most part of isolated silanol groups were consumed to make a chemical bond with the pyridyl groups of 3-PySi(OEt)₃.

The solid state ²⁹Si CP-MAS NMR spectra of Py_FSM-16 (Figure 3) had the resonances corresponding to RSiOH(OSi)₂ i.e. T² and RSi(OSi)₃ i.e. T³, which were not obtained before the modification with 3-PySi(OEt)₃. This demonstrates that bidentate and tridentate pyridyl groups are immobilized on FSM-16 as shown in Figure 4. On the basis of the above results and the molecular size of 3-PySi(OEt)₃, it is likely that the pyridyl group is slightly-inclined against the surface of FSM-16.

Table 1 shows the activities of Py_FSM-16, FSM-16, and MgO in the aldol condensation and Tishchenko reaction of butanal. In this reaction, the dimer

(2-ethyl-3-hydroxyhexanal) resulting from the aldol reaction and the trimers (2-ethyl-3-hydroxyhexyl butyrate) resulting from the Tishchenko reaction of the dimer with butanal were obtained as shown in Scheme 1. For the aldol reaction, the presence of only basic sites is sufficient, but for the Tishchenko reaction, the presence of both basic and acidic sites is required [21-24]. It is believed that the oligomers were formed through condensation and acetalization catalyzed by the acidic sites. FSM-16 formed a large amount of oligomers (mainly tetramers), indicating that the surface OH groups of FSM-16 acted as acidic sites [25]. Through the use of Py_FSM-16, the reaction was selective for the formation of dimers by aldol condensation, and the Tishchenko reaction was significantly suppressed (Entries 2 and 3). Through the homogeneous modification of the acidic OH group of FSM-16 with pyridyl groups, basic sites are generated within the interior of the uniform and well-ordered mesopore of FSM-16 and the acidic sites are suppressed. Therefore, the selectivity of the dimer was remarkably improved. This result strongly suggests that the uniform and well-ordered basic nanospace is synthesized by the homogeneous modification with the pyridyl groups. In contrast, in the case of MgO which is a typical solid base, a remarkable amount of trimer was obtained in addition to dimer. This result strongly suggests that both the acidic and basic sites of MgO participate in the Tishchenko reaction.

When the oxidative coupling polymerization of 2,5-dimethylphenol was catalyzed by the copper-pyridine complex immobilized catalyst (Cu/Py_FSM-16), no additive such as aliphatic amines, pyridine or alkyl-substituted pyridine was used. Cu/Py_FSM-16 gave an off-white powder, whereas a conventional catalyst (CuCl(I) with a pyridine homogeneous system (the molar ratio of copper to pyridine is 0.5) [26-28] provided a yellow-brown polymer. The conversion rate of 2,5-dimethylphenol over Cu/Py_FSM-16 was slower than that of conventional CuCl(I) with a pyridine homogeneous system. This may be due to the limit of diffusion of 2,5-dimethylphenol and the oligomer in the narrow mesoporous interior (2.08 nm). Figure 5 shows the ^1H NMR spectra of polyphenylene ether obtained by (a) a conventional CuCl(I)/pyridine system for 3 h and (b) Cu/Py_FSM-16 for 15 h. Cu/Py_FSM-16 gave two sharp signals at 2.2 and 6.5 ppm with very small peaks due to the terminal units, indicating that a high regioselective polymerization had proceeded. On the contrary, the conventional CuCl(I)/pyridine system gave broad signals around 2.2 and 6.5 ppm. This indicates that unfavorable branching polymers were formed. These results indicate that the copper-pyridine system promotes the oxidative coupling polymerization of 2,5-dimethylphenol and that the one-dimensional and uniform mesoporous channel of FSM-16 effectively restricted the molecular orientation, resulting

in a high regioselectivity upon coupling.

4. Conclusion

In conclusion, we synthesized basic nanospace by homogeneous modification of mesoporous silica (FSM-16) with 3-(triethoxysilyl)pyridine. The aldol reaction of butanal to dimer (2-ethyl-3-hydroxyhexanal) selectively proceeded over Py_FSM-16 and Tishchenko reaction to trimer was inhibited. This indicates that the synthesized basic nanospace can act as a novel effective solid base catalyst with molecular shape selectivity and molecular recognition ability. The copper-pyridine complex was immobilized within the interior of FSM-16 by using a pyridyl group as a ligand. The copper-pyridine complex was immobilized within the interior of FSM-16 gave a high regioselectivity in the oxidative coupling polymerization of 2,5-dimethylphenol without additives, indicating that the one-dimensional and uniform mesoporous channel effectively restricted the molecular orientation.

Acknowledgments

The high-purity water glass was kindly supplied from Fuji Silysia Chem. Co. Ltd. TS

acknowledges the Grant-in-Aid for Scientific Research for Young Researchers (B) (No. 21760627) under Ministry of Education, Culture, Sports Science and Technology (MEXT) of Japan. KT is supported by Program for Improvement of Research Environment for Young Researchers from Special Coordination Funds for Promoting Science and Technology (SCF) commissioned by the Ministry of Education, Culture, Sports, Science and Technology (MEXT) of Japan.

References

- [1] Hoffmann F., Cornelius M., Morell J., Froba M. (2006) *Angew. Chem. Int. Ed.* 45: 3216.
- [2] Stein A., (2003) *Adv. Mater.* 15: 763.
- [3] Stein A., Melde B. J., Schrodin R. C. (2000) *Adv. Mater.*, 12: 1403.
- [4] Wight A. P., Davis (2002) *Chem. Rev.*, 102: 3589.
- [5] Taguchi A., Schuth F. (2005) *Microporous Mesoporous Mater.*, 77: 1.
- [6] Tajima K. and Aida T. (2000) *Chem Commun.*, 24: 2399.
- [7] Kageyama K., Tamazawa J., Aida T. (1999) *Science*, 285: 2113.
- [8] Lin V. S.-Y., Radu D. R., Han M.-K., Deng W., Kuroki S., Shanks B. H., Pruski M. (2002) *J. Am. Chem. Soc.*, 124: 9040.
- [9] Shibasaki Y., Nakamura M., Ishimaru R., Kondo J. N., Domen K., Ueda M. (2004) *Macromolecules*, 37: 9657.
- [10] Shibasaki Y., Nakamura M., Ishimaru R., Kondo J. N., Ueda M. (2005) *Chem. Lett.*, 34: 662.

- [11] Inagaki S., Guan S., Fukushima Y., Ohsuga T., Terasaki O. (1999) *J. Am. Chem. Soc.*, 121: 9611.
- [12] Inumaru K., Inoue Y., Kakii S., Nakao, T., Yamanaka S. (2004) *Phys. Chem. Chem. Phys.* 6: 3133.
- [12] Inagaki S., Guan S., Ohsuga T., Terasaki O. (2002) *Nature*, 416: 304.
- [13] Feng Y-F., Yang X.-Y., Di Y., Du Y.-C., Zhang Y.-L., Xiao F.-S., (2006) *J. Phys. Chem. C*, 110: 14142.
- [14] Shimizu K., Hayashi E., Hatamachi T., Kodama T., Higuchi T. Satsuma A., Kitayama Y., (2005) *J. Catal.*, 231: 131.
- [15] Nakajima K., Tomita I., Hara M., Hayashi S., Domen K., Nomura J. K. (2005) *J. Mater. Chem.*, 15: 21362.
- [16] Rao Y. V. S., De Vos D.E., Jacobs P. A., (1997) *Angew. Chem. Int. Ed.* 36: 2661.
- [17] Weitkamp J., Hunger M., Ryma U., (2001) *Microporous Mesoporous Mater.*, 48: 255.
- [18] Pines R. H., in *The Chemistry of Catalytic Hydrocarbon Conversions*, Academic Press, New York, (1981) 123.
- [19] Inagaki S., Koiwai A., Suzuki N., Fukushima Y., Kuroda K., (1996) *Bull. Chem. Soc. Jpn.*, 69: 1449.

- [20] Reidmiller F., Jockisch A., Schmidbaur H., (1998) *Organometallics*, 17: 4444.
- [21] Tanabe K., and Saito K., *J. Catal.*, (1974) 35: 274.
- [22] (a) Hattori H., (1995) *Chem. Rev.*, 95: 537, (b) Hattori, H. (2001) *Appl. Catal. A: General*, 222: 247, (c) Seki, T. and Hattori, H., (2003) *Catal. Surv. Asia*, 7: 145.
- [23] Tsuji H., Yagi F., Hattori H., (1994) *J. Catal.*, 148: 759.
- [24] Seki T., Nakajo T., Onaka T., (2006) *Chem. Lett.*, 35: 824.
- [25] (a) Yamamoto T., Tanaka T., Funabiki T., and Yoshida S. (1998) *J. Phys. Chem. B*, 102: 5830, (b) Yamamoto T., Tanaka T., Inagaki, S., Funabiki T., and Yoshida S. (1999) *J. Phys. Chem. B*, 103: 6450.
- [26] Sheldon R. A. and Kochi J. K., in *Metal Catalyzed Oxidation of Organic Compounds*, Academic Press, New York (1981) 369.
- [27] Shimizu M., Watanabe Y., Orita H., Hayakawa T., Takehira K., (1993) *Bull. Chem. Soc. Jpn.*, 66: 251.
- [28] Takehira K., Shimizu M., Watanabe Y., Orita H., Hayakawa T., (1989) *J. Chem. Soc., Chem. Commun.*, 1705.

Table 1. Catalytic activities of the aldol condensation and the Tishchenko reaction of butanal

Entry	Catalysts	Conv.	Sel. (%)
-------	-----------	-------	----------

		(%)	dimer ^e	trimer ^f	ester ^g	oligomer
1	FSM-16 ^{a,b}	33.7	42.4	3.0	0.8	53.6
2	Py_FSM-16 ^{a,b}	16.5	82.2	10.3	2.0	trace
3	Py_FSM-16 ^{a,c}	51.5	84.5	10.1	0.7	trace
4	MgO ^{a,d}	50.5	49.5	38.6	10.7	trace

a 7 mmol butanal

b 393K, 24 h, The catalyst was evacuated at 423 K for 1h before the reaction.

c 393K, 72 h, The catalyst was evacuated at 423 K for 1h before the reaction.

d 323 K, 1h, The catalyst was evacuated at 773 K for 1 h before the reaction.

e 2-ethyl-3-hydroxyhexanal, f 2-ethyl-3-hydroxyhexyl butyrate, g butyl butyrate

Figure captions

Figure 1. (A) N₂ adsorption-desorption isotherms and (B) BJH pore distributions of (a) FSM-16 and (b) Py_FSM-16, R_p : radius of pore size.

Figure 2. FT-IR spectra of (a) 3-(triethoxysilyl)pyridine, (b) FSM-16 and (c) Py_FSM-16

Figure 3. ²⁹Si CP-MAS NMR spectra of (a) FSM-16 and (b) Py_FSM-16

Figure 4. Structure of immobilized 3-(triethoxysilyl)pyridine (a) tridentate and (b) bidentate

Figure 5. ¹H NMR spectra of poly[oxy-2,5-dimethyl(1,4-phenylene)] obtained by (a) conventional CuCl-pyridine and (b) Cu/Py_FSM-16

Scheme 1. Aldol condensation and Tishchenko reaction of butanal

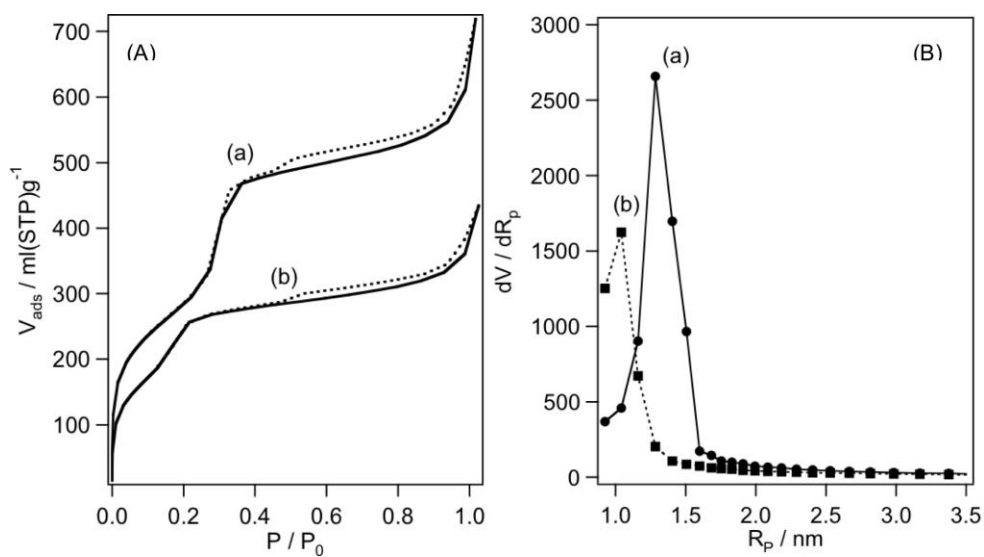


Figure 1. (A) N_2 adsorption-desorption isotherms and (B) BJH pore distributions of (a) FSM-16 and (b) Py_FSM-16, R_p : radius of pore size.

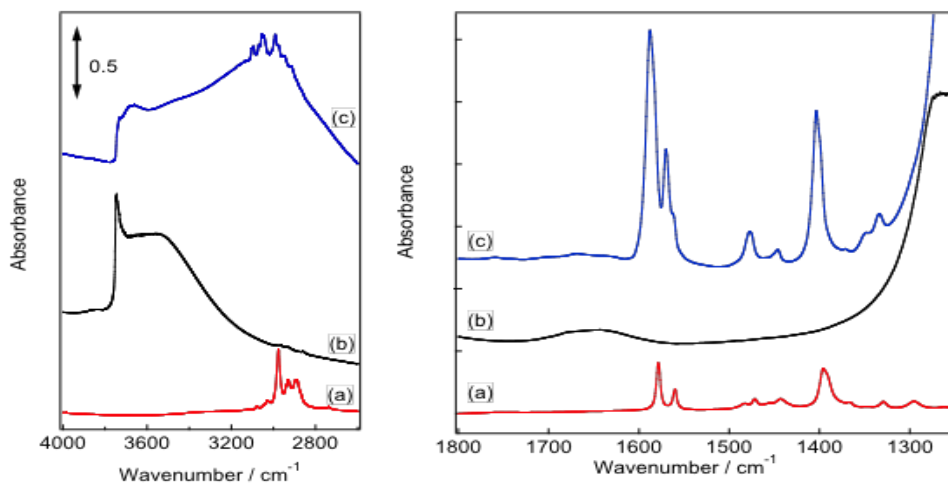


Figure 2. FT-IR spectra of (a) 3-(triethoxysilyl)pyridine, (b) FSM-16 and (c) Py_FSM-16

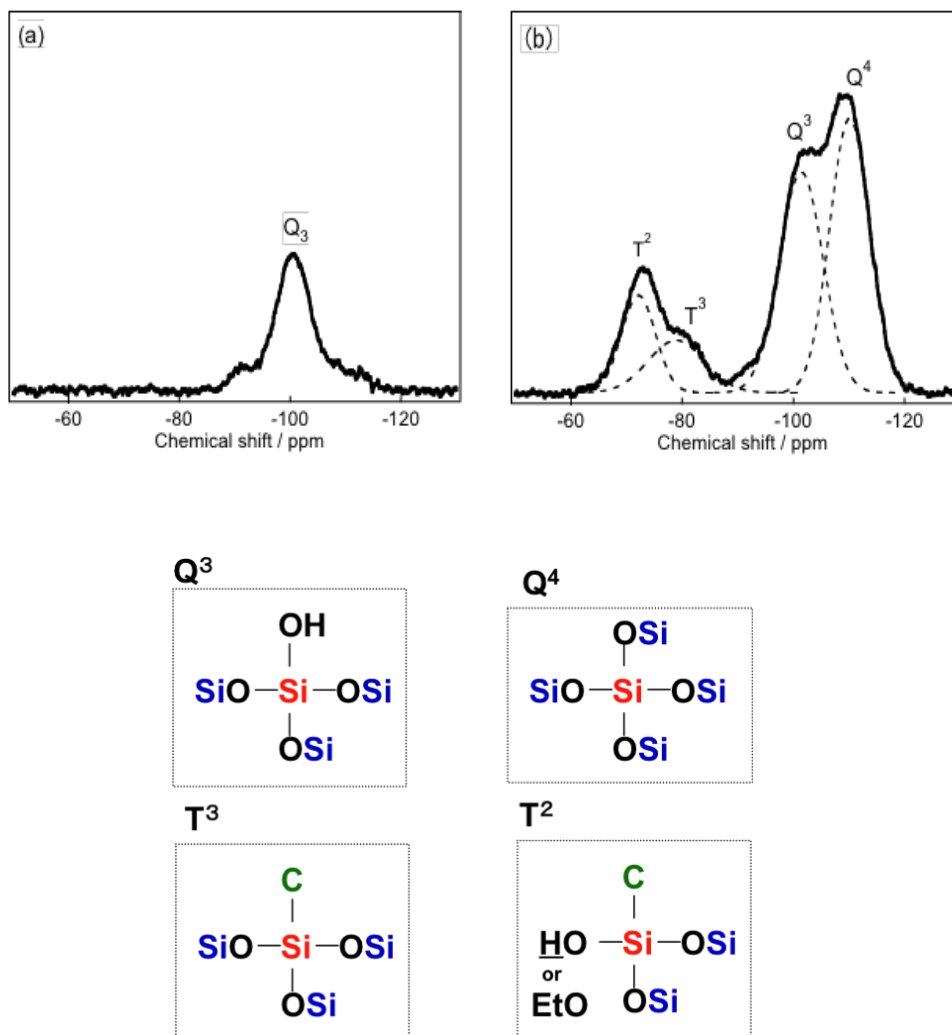


Figure 3. ^{29}Si CP-MAS NMR spectra of (a) FSM-16 and (b) Py_FSM-16

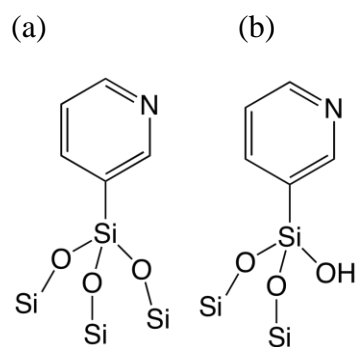


Figure 4. Structure of immobilized 3-(triethoxysilyl)pyridine (a) tridentate and (b) bidentate

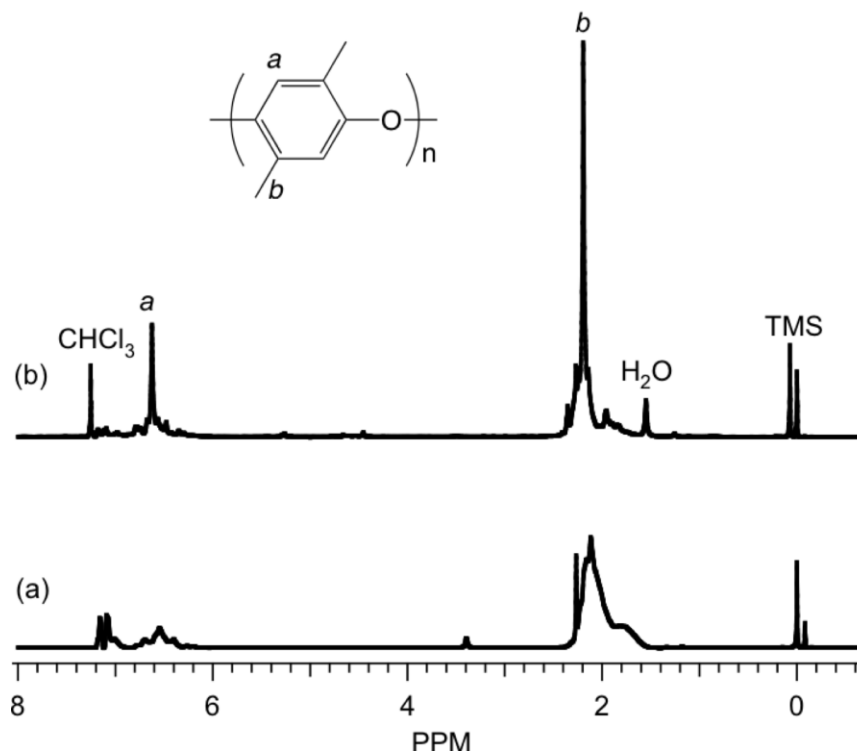
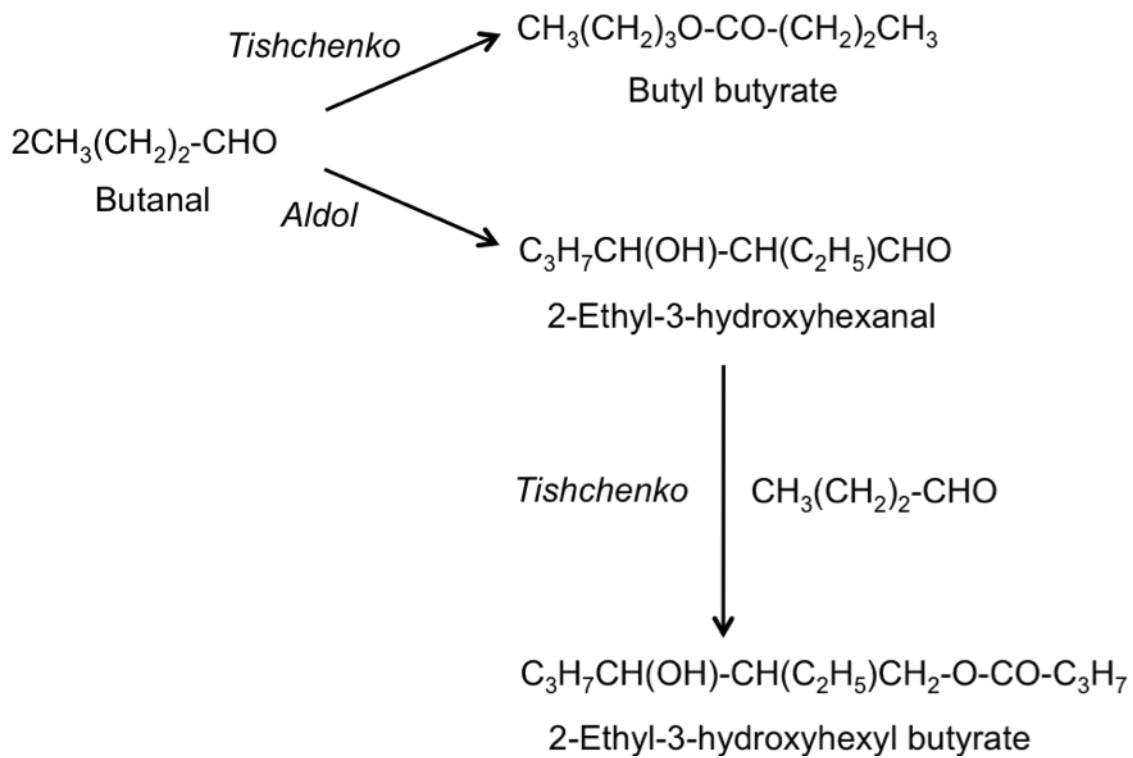


Figure 5. ¹H NMR spectra of poly[oxy-2,5-dimethyl(1,4-phenylene)] obtained by (a) conventional CuCl-pyridine and (b) Cu/Py_FSM-16



Scheme 1. Aldol condensation and Tishchenko reaction of butanal